PNAS RESEARCH ARTICLE | GENETICS OPEN ACCESS

Leveraging a natural murine meiotic drive to suppress invasive populations

Luke Gierus[a,b,1], Aysegul Birand[c,1], Mark D. Bunting[a,b], Gelshan I. Godahewa[b,d], Sandra G. Piltz[a,b], Kevin P. Oh[e,f], Antoinette J. Piaggio[g], David W. Threadgill[h], John Godwin[i], Owain Edwards[e,j], Phillip Cassey[c], Joshua V. Ross[k], Thomas A. A. Prowse[c] and Paul Q. Thomas[a,b,2]

Edited by James Bull, University of Idaho, Moscow, ID; received August 3, 2022; accepted October 4, 2022

Invasive rodents are a major cause of environmental damage and biodiversity loss, particularly on islands. Unlike insects, genetic biocontrol strategies including population-suppressing gene drives with biased inheritance have not been developed in mice. Here, we demonstrate a gene drive strategy (t_{CRISPR}) that leverages super-Mendelian transmission of the *t* haplotype to spread inactivating mutations in a haplosufficient female fertility gene (*Prl*). Using spatially explicit individual-based in silico modeling, we show that t_{CRISPR} can eradicate island populations under a range of realistic field-based parameter values. We also engineer transgenic t_{CRISPR} mice that, crucially, exhibit biased transmission of the modified *t* haplotype and *Prl* mutations at levels our modeling predicts would be sufficient for eradication. This is an example of a feasible gene drive system for invasive alien rodent population control.

genetic biocontrol | gene drive | invasive rodents | conservation | modeling

Significance

Invasive rodents pose a significant threat to global biodiversity, contributing to countless extinctions, particularly on islands. Genetic biocontrol has considerable potential to control invasive populations but has not been developed in mice. Here, we develop a suppression gene drive strategy for mice that leverages a modified naturally occurring element with biased transmission to spread faulty copies of a haplosufficient female fertility gene (t_{CRISPR}). In silico modeling of island populations using a range of realistic parameters predicts robust eradication. We also demonstrate proof of concept for this strategy in laboratory mice. This work marks a significant step toward the development of a gene drive for the suppression of invasive mice.

Invasive mammalian pests are among the greatest threats to global biodiversity and have constituted an unprecedented form of global change (1, 2). Commensal rodents, including house mice (*Mus musculus*), have spread throughout the globe, causing significant environmental damage and loss of agricultural productivity (3, 4). Islands are biodiversity hotspots and are particularly susceptible to the impact of invasive rodents, where they contribute to widespread extinction and endangerment, particularly of migratory bird species, reptiles, and plant stocks that have not evolved with rodents (5–9). Current control methods rely principally on the widespread distribution of anticoagulant rodenticides, an approach that is costly to apply at scale, carries ethical concerns regarding the mechanism of toxicity, and is not species specific, rendering its application feasible only on islands without significant human population, livestock, or sensitive off-target species (10).

Genetic biocontrol technologies including gene drives offer the potential for landscape-scale modification or suppression of invasive populations (11). Gene drives are natural or synthetic genetic elements that spread through a population via super-Mendelian transmission. Building upon the pioneering concepts of Austin Burt (12) and others (13) and leveraging the emergence of CRISPR-Cas9 gene editing technology (14), synthetic "homing" gene drives have recently been developed in several insect species, including *Anopheles* malaria vectors (15–18). However, in mice, homing gene drives have been challenging to develop (19–21), prompting us to consider alternative strategies. First described in 1927 (22), the *t* haplotype is a naturally occurring gene drive element commonly found in wild mouse populations that functions as a male meiotic drive, biasing transmission from carrier males by up to ~95%, depending on the variant (23, 24). In nonlethal *t* haplotype variants such as t^{w2}, homozygous males are sterile and homozygous females are viable and fertile (25). Earlier modeling studies suggested that nonlethal *t* haplotypes could cause eradication in small populations due to male sterility (25, 26). However, the fact that the nonlethal *t* haplotype is still observed in natural populations (13 to 55%) (27) suggests that there is selection against it in the form of reduced fertility or viability. There is some evidence that polyandry (i.e., mating with multiple males per breeding cycle) reduces lethal *t* haplotype frequencies due to sperm competitive disadvantage (28), which could also apply to t^{w2} (28–31).

Given the significant bias in *t* transmission, it is possible that this natural male meiotic drive could be leveraged for mouse population suppression or even eradication on islands (4). Here, we describe a gene drive strategy termed t_{CRISPR}, in which fertile females are progressively depleted due to a CRISPR transgene embedded in the *t* haplotype that targets a haplosufficient female fertility gene. Using spatially explicit individual-based in silico modeling on a hypothetical island, we demonstrate that t_{CRISPR} has eradication potential across a range of realistic scenarios. We further demonstrate the feasibility of this strategy by engineering and testing t_{CRISPR} in a genetically contained "split drive" format, where the Cas9 and guide RNA (gRNA) expression cassettes are integrated into different chromosomes.

Author contributions: L.G., A.B., and P.Q.T. designed research; L.G., A.B., M.D.B., G.I.G., S.G.P., K.P.O., A.J.P., O.E., P.C., J.V.R., T.A.A.P., and P.Q.T. performed research; D.W.T. and J.G. contributed new reagents/analytic tools; L.G., A.B., M.D.B., G.I.G., S.G.P., K.P.O., A.J.P., D.W.T., J.G., O.E., P.C., J.V.R., T.A.A.P., and P.Q.T. analyzed data; and L.G., A.B., and P.Q.T. wrote the paper.

The authors declare no competing interest.

This article is a PNAS Direct Submission.

See online for related content such as Commentaries.

[1]L.G. and A.B. contributed equally to this work.

[2]To whom correspondence may be addressed. Email: paul.thomas@adelaide.edu.au.

This article contains supporting information online at http://www.pnas.org/lookup/suppl/doi:10.1073/pnas.2213308119/-/DCSupplemental.

Published November 8, 2022.

Results

In Silico Spatial Modeling Demonstrates the Eradication Potential of t_{CRISPR}. Given the significant transmission bias of the *t* haplotype, we investigated whether this could be harnessed to develop a synthetic CRISPR gene drive targeting a haplosufficient gene required for female fertility [e.g., Prolactin, *Prl* (32)]. We envisaged a system whereby mutations in *Prl* are generated in the male germline through activation of a Cas9/gRNA transgene embedded in a nonlethal *t* variant such as t^{w2} (which is transmitted to ~95% of offspring (33) by heterozygous males) (t_{CRISPR}; Fig. 1 *A* and *B*). To assess the population suppression potential of the t_{CRISPR} strategy, we performed spatially explicit individual-based simulations (see Fig. 2 for sample simulations), which demonstrated that t_{CRISPR} can effectively eradicate large populations (N ~200,000) of mice (Figs. 2a and 3).

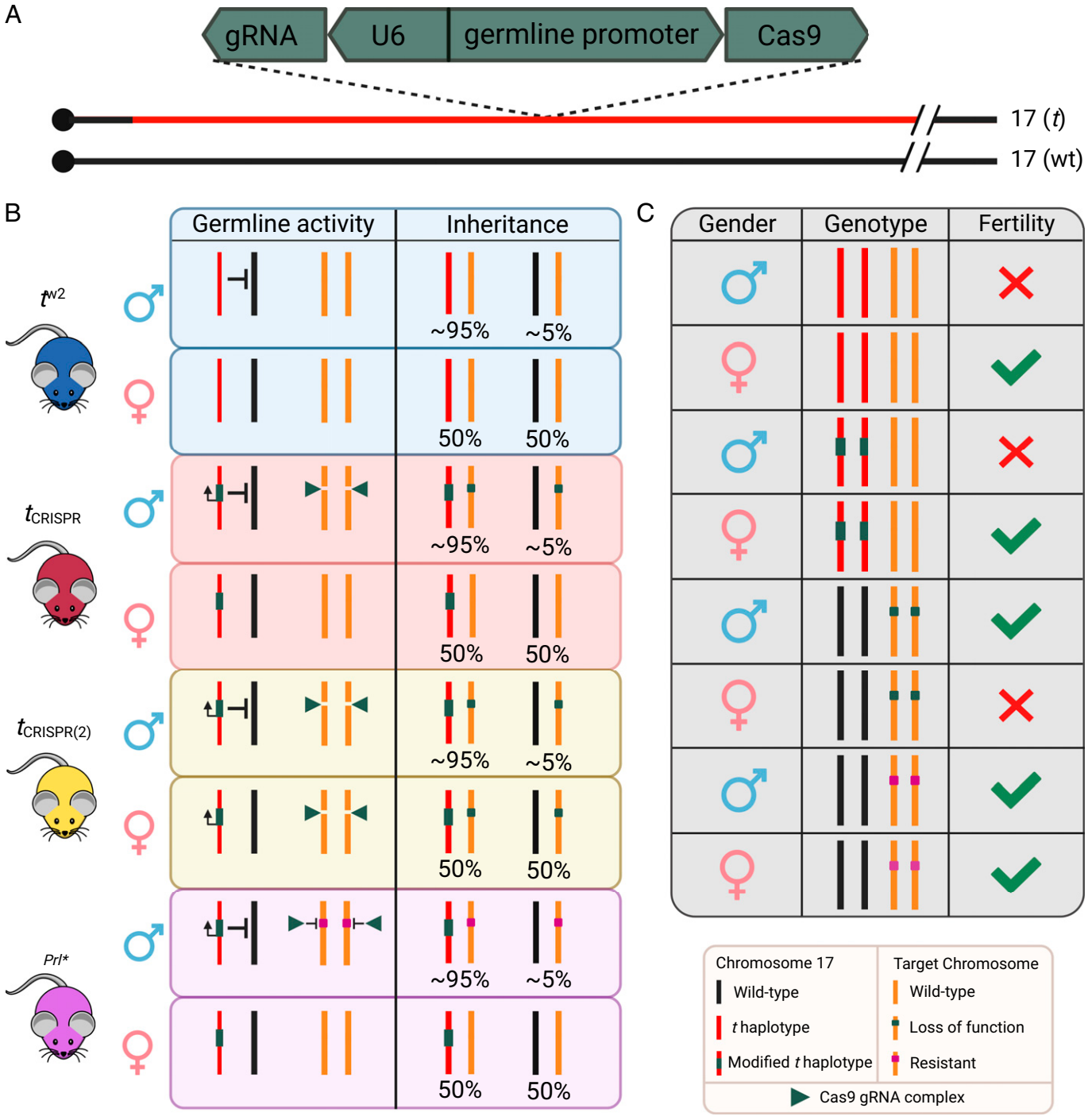

Fig. 1. Overview of *t* haplotype modification strategies for population suppression. (*A*) The integration of a transgene within the *t* haplotype expressing Cas9 under the control of a male-specific promoter or a germline-specific promoter, coupled with a ubiquitously expressed gRNA targeting a haplosufficient female fertility gene. (*B*) Inheritance of t^{w2} is biased in males but not females. In the t_{CRISPR} system, Cas9 is only active in males and, with a ubiquitously expressed gRNA, disrupts a haplosufficient female fertility gene in the germline. t_{CRISPR} males transmit the t_{CRISPR} transgene and a disrupted fertility gene to ~95% and 100% of offspring, respectively. The $t_{CRISPR(2)}$ strategy is identical except that the Cas9 is active in the male and female germline, thereby generating a more rapid increase in female infertility alleles. *Prl** mice contain a sequence difference at the gRNA target site but maintain a functional protein, making these mice resistant against any further cleavage at that site. (*C*) Fertility of male and female mice carrying the various versions of chromosome 17 and *Prl* within the target chromosome.

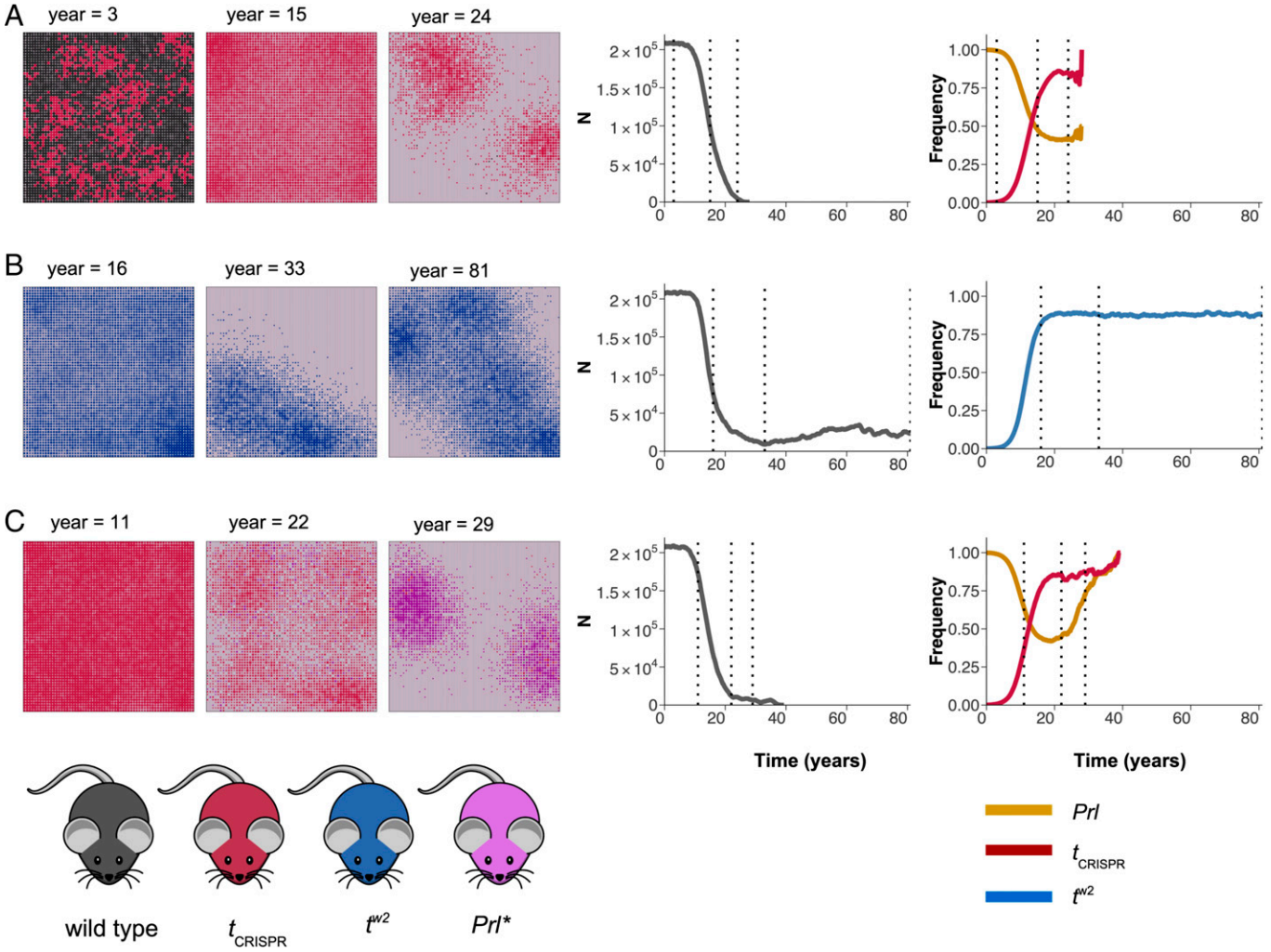

Fig. 2. Sample simulations using two strategies, namely, t_{CRISPR} and t^{w2}. Shown in order are three snapshots of the spatial distribution of mouse populations, total population size, and the allele frequency change through time, starting with the inoculation of *t* haplotype individuals at year = 0 (dashed lines in the plots correspond to the years of the snapshots). Each circle represents the population in that patch, the circle size is proportional to the patch population size, and the circle color represents the most abundant *t* haplotype in that patch. Empty patches appear as light gray (Movies S1–S3 and *SI Appendix*, Table S1 contain the base values and the abbreviations of the parameters). (*A*) t_{CRISPR} spread across the entire landscape in ~10 y, and substantial suppression of the population was achieved after 21 y with complete eradication in 28.1 y. Functional prolactin frequency declined steadily in the population following inoculation with t_{CRISPR} individuals. (*B*) t^{w2} spread across the entire landscape in similar time frames to t_{CRISPR}, but eradication of the population was not achieved. (*C*) When the probability of loss of function after a successful DNA cut is reduced to $p_L = 0.9996$, resistant genotypes (*Prl**) emerged in ~20 y after inoculation and functional prolactin levels started to increase, but eradication was still successful ($p_m = 0.63$ in all three simulations; other parameters, if not stated, are given in *SI Appendix*, Table S1).

Typically, during the first decade after inoculation, t_{CRISPR} spread across the entire landscape, *Prl* (functional) allele frequency declined steadily, and substantial (> 90%) suppression of the population was achieved in ~20 y (e.g., Fig. 2*A*), with complete eradication in ~28 y. Simulated eradication using t_{CRISPR} was successful across a wide range of parameters related to gene drive efficiency and mouse life history, often with shorter time to eradication (see below). t^{w2} can also affect population suppression through sterility of male homozygotes (e.g., Fig. 2*B*); however, simulated eradication probability was much lower compared to t_{CRISPR}, and when eradication was successful, the time to eradication was substantially longer (Fig. 3). Time to eradication for t_{CRISPR} was slightly longer than other proposed gene-drive strategies such as a homing drive for female infertility and a driving Y X-shredder (34–36) (*SI Appendix*, Fig. S1).

Effects of t haplotype transmission and multiple mating probabilities. The transmission probability of the *t* haplotype in heterozygous males (p_t) and the probability of multiple mating (p_m) strongly influenced t_{CRISPR} eradication probability (Fig. 3*A*) and time to eradication (Fig. 3*B*). Eradication is successful when $p_t \geq 0.93$ with moderate levels of polyandry ($p_m = 0.46$). Higher levels of polyandry or sperm competition require higher transmission efficiencies (p_t) for successful eradication. With these parameter values, t^{w2} produced very low probabilities of eradication. In contrast, when $p_t = 0.95$, t_{CRISPR} successfully eradicated at all levels of polyandry tested ($p_m = 0.46, 0.63, 0.8$) when sperm competition was moderate ($d_s = 0.17$) and at moderate levels of polyandry when sperm competition was very high ($d_s = 0.39$). In addition, time to eradication was much shorter with t_{CRISPR} than with t^{w2} (~25 y and ~43 y for t_{CRISPR} and t^{w2}, respectively, when $p_m = 0.46$, $d_s = 0.17$; Fig. 3*B*). t_{CRISPR} also achieved stronger population suppression than t^{w2} when eradication failed for both strategies (Fig. 3*C*).

Effect of CRISPR-Cas9 efficiency. The probability of a successful DNA cut (p_C, cutting efficiency) had an unexpected effect on simulation outcomes where less efficient cutting (e.g., $p_C = 0.8$) resulted in a higher probability of eradication and shorter time to

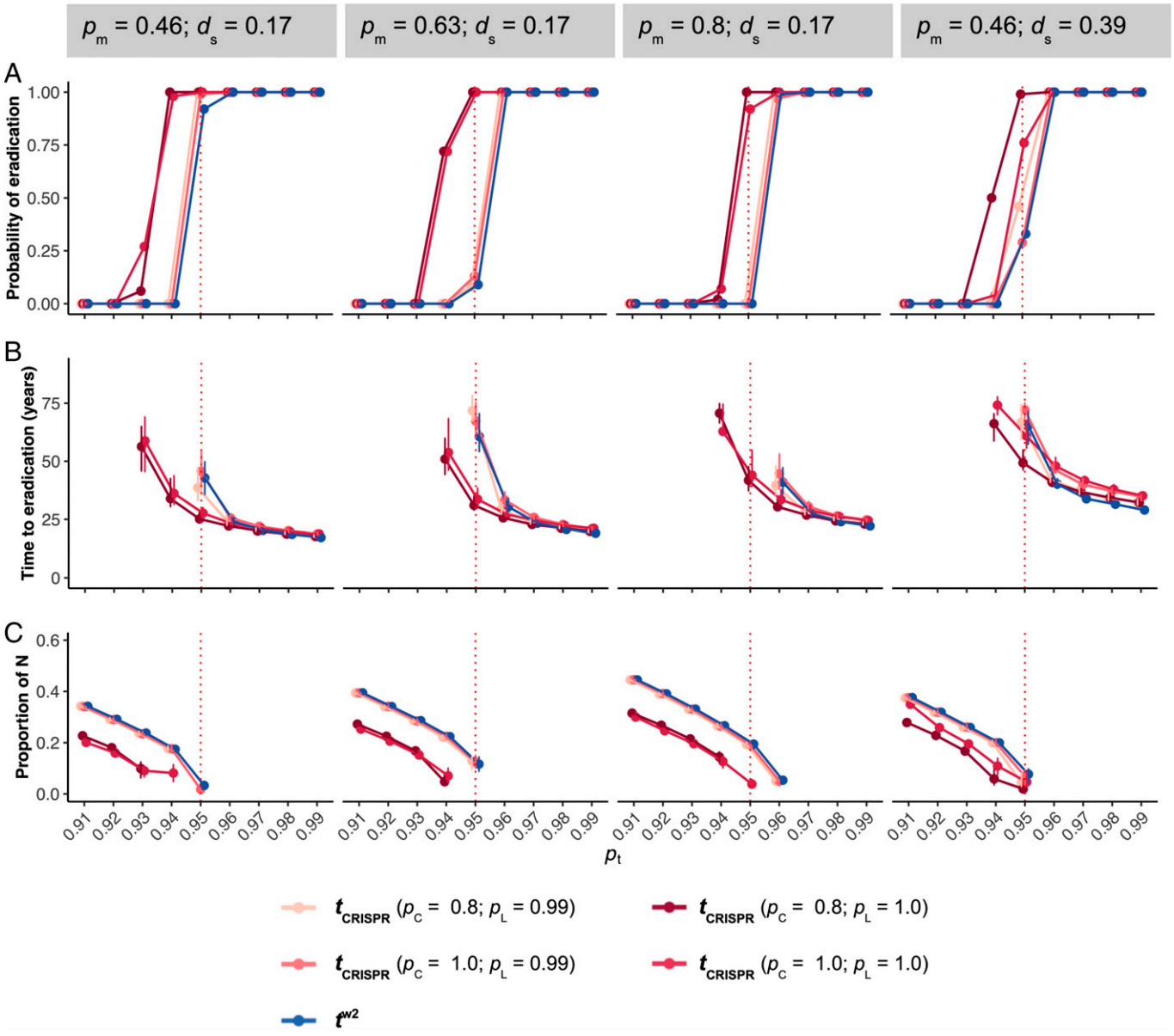

Fig. 3. Effect of p_t on the success of the t^{w2} and t_{CRISPR} elimination strategies. (*A*) The probability of eradication; the median with interquartile ranges of the time to eradication (*B*), and the proportion of remaining population sizes when eradication was unsuccessful (*C*) based on 100 simulations for each parameter combination (18,000 simulations in total). Higher values of p_t lead to higher probabilities of eradication, shorter times to eradication, and higher population suppression when eradication failed, whereas high levels of either sperm competition (d_s = 0.39) or polyandry (p_m = 0.8) reduced eradication probabilities and delayed times to eradication except when p_t was very high (*B*). Eradication failed for both strategies when sperm competition and polyandry are very high (results not shown when $p_m \geq 0.63$ and d_s = 0.39). Compared to t^{w2}, t_{CRISPR} generally had higher eradication probabilities, shorter eradication times, and higher population suppression when eradication failed. At p_t = 0.95 (dashed line), t_{CRISPR} was always successful if there was a complete loss of function (p_L = 1) after a successful DNA cut (other parameters, if not stated, are given in *SI Appendix*, Table S1).

eradication than p_C = 1.0 (Fig. 3 and *SI Appendix*, Fig. S2). In contrast, a high probability of loss of gene function (p_L) following a successful cut is required to prevent resistant alleles that retain function from emerging (e.g., Fig. 2*C* with p_C = 0.8 and p_L = 0.9996). Typically, once functional resistant genotypes emerged, the decline in *Prl* frequency was rapidly reversed. However, in most cases, eradication was still achieved with t_{CRISPR} when $p_L < 1$ (*SI Appendix*, Fig. S2). t_{CRISPR} continued to outperform t^{w2} for all values of p_C and p_L when polyandry and sperm competition were moderate and when $p_C < 0.95$ for higher values of polyandry and sperm competition. This suggests that eradication was achieved mostly through male sterility; however, female infertility continued to contribute to eradication (*SI Appendix*, Fig. S2). When p_L was reduced even further to 0.99, the contribution of female infertility declined and t_{CRISPR} behaved more like t^{w2} with a similar probability of eradication and time to eradication (Fig. 3).

Sensitivity analysis predictions support brute-force simulations. The predictions from the Boosted Regression Tree model, fitted to the sensitivity-analysis results, support the above predictions (Fig. 4 and *SI Appendix*, Fig. S3). t_{CRISPR} was predicted to successfully eradicate for a wide range of transmission probabilities ($p_t \geq 0.93$) and polyandry ($p_m > 0.2$) when sperm competition was moderate (d_s = 0.17, Fig. 4*A*; also see *SI Appendix*, Fig. S4*A*). When p_t = 0.95, t_{CRISPR} was predicted to successfully eradicate and could tolerate higher levels of both sperm competition and polyandry, whereas t^{w2} was successful only for low levels of polyandry ($p_m < 0.4$; Fig. 4*B* and *SI Appendix*,

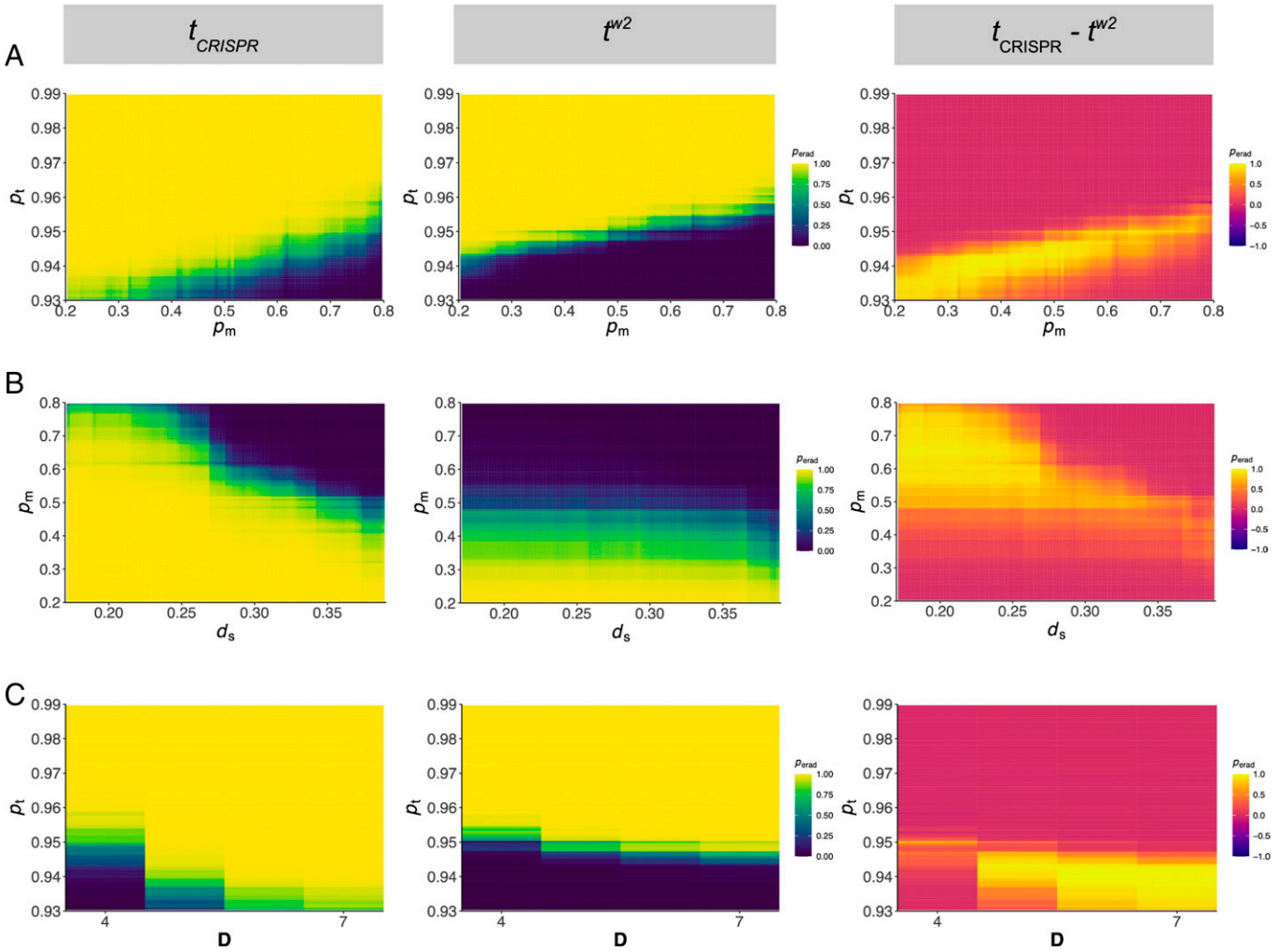

Fig. 4. Predicted probabilities of eradication based on BRT fitted to sensitivity-analysis results. Shown are the probabilities of eradication using t_{CRISPR} (*Left*) and t^{w2} (*Middle*) and their difference (*Right*; note the scale change to [−1, 1]). (*A*) t_{CRISPR} was predicted to be successful in eradication for less efficient transmission ($p_t < 0.95$) together with low to moderate levels of polyandry ($p_m < 0.46$), where t^{w2} failed (assuming moderate sperm competition, $d_s = 0.17$). At $p_t = 0.95$, t_{CRISPR} was predicted to be successful for a wide range of p_m. (*B*) The expected probability of eradication was very low with t^{w2} for $p_m > 0.40$ and zero for $p_m > 0.60$ irrespective of levels of sperm competition (assuming $p_t = 0.95$). t_{CRISPR} had higher probabilities of eradication for higher levels of polyandry, unless sperm competition was very high. (*C*) Dispersal distances, $D \geq 5$ increased eradication probabilities for t_{CRISPR} when $p_t \leq 0.95$, but not for t^{w2} (assuming $p_m = 0.46$). Other parameters, if not stated, are given in *SI Appendix*, Table S1.

Fig. S4*B*). Increasing dispersal distance (D) increased eradication probabilities for t_{CRISPR} when $p_t < 0.96$ but not for t^{w2} (Fig. 4*C* and *SI Appendix*, Fig. S4*C*). Lower p_t and higher levels of polyandry and sperm competition delayed the time to eradication for both strategies (*SI Appendix*, Fig. S5); however, t_{CRISPR} had a shorter time to eradication than t^{w2} for all values of polyandry and sperm competition when $p_t \leq 0.95$.

The role of fertile females. We also investigated eradication probability with a related strategy ($t_{CRISPR(2)}$) in which Cas9 is active in the germline of both males and females (Fig. 1*B* and *SI Appendix*, Fig. S6). Although *Prl* is not required in the female germline, inactivation of *Prl* in females ultimately caused a critical shortage of fertile females carrying the *t* haplotype (*SI Appendix*, Fig. S6*B*), which limited drive spread. Given that the *t* haplotype is present in some wild populations, we also modeled the impact of endogenous t^{w2} in the target population on the eradication success of t_{CRISPR}. Since *Prl* prevalence is reduced after the introduction of the drive, t_{CRISPR} was at a disadvantage with fewer fertile females spreading the drive compared to the naturally occurring *t* haplotypes (e.g., *SI Appendix*, Fig. S7*A*). Encouragingly, an analysis of previously published pooled whole-genome sequence (pool-seq) datasets (37) ($n = 40$ individuals per island) for reads mapping to diagnostic transcripts detected no evidence of *t* haplotypes among mice sampled from four islands in Western Australia, the north Pacific, and the western coast of North America (*SI Appendix*, Fig. S8). In contrast, one of the four continental populations in the same study showed evidence of *t* haplotypes, with the number of reads mapped exceeding the expected values at the lowest detectable *t* haplotype frequency (i.e., a single *t* haplotype sampled). Interestingly, our results also suggest that the competitive advantage of naturally occurring *t* haplotypes over t_{CRISPR} could allow them to be used as "rescue drives," albeit only under a limited range of parameter values (e.g., *SI Appendix*, Fig. S7*B*).

Other parameters. Initial population size on the island did not affect time to eradication when either the population density or the island size was altered (*SI Appendix*, Fig. S9), suggesting that the length and the number of breeding cycles in a year, along with dispersal abilities, influence the temporal dynamics of the drive. Lastly, if *t*-carrying females preferred wild-type males over *t*-carrying males, eradication probability reduced

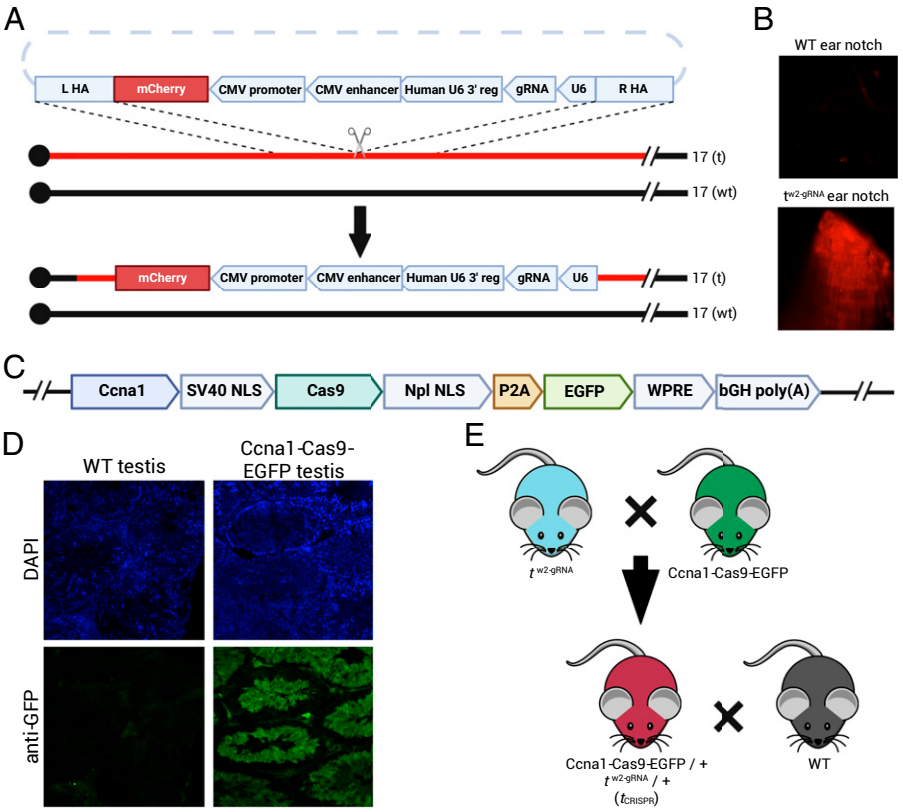

Fig. 5. Generation and characterization of split drive t_{CRISPR} mice. (*A* and *B*) Insertion of the gRNA and mCherry expression cassettes into the t haplotype using homologous recombination. $t^{w2\text{-}gRNA}$ mice were genotyped by site specific PCR and mCherry fluorescence. WT, wild type. (*C*) Construct used to generate the Ccna1-Cas9-EGFP mice. (*D*) DAPI (blue) and EGFP (green) immunofluorescence in adult testes correlated to Cas9 expression controlled by the Ccna1 promoter. (*E*) Split drive breeding strategy to generate transhemizygous t_{CRISPR} mice.

and time to eradication increased (*SI Appendix*, Fig. S10); however, t_{CRISPR} had better eradication success than t^{w2}. Together, these predictions indicate that the t_{CRISPR} strategy has robust eradication potential across a range of realistic parameter values.

Generation and Analysis of a t_{CRISPR} Split Drive System. To assess the feasibility of the t_{CRISPR} strategy, we sought to generate and test a t_{CRISPR} drive under laboratory conditions. To ensure containment, we employed a split drive design whereby a constitutive gRNA expression cassette was integrated into the t^{w2} locus and a male germline Cas9 expression cassette was inserted at a different genomic location. We selected *Prl* for the gRNA target as the function of this haplosufficient female-specific fertility gene is well characterized (32). Six gRNAs targeting PRL essential amino acids (38–42) (P2.1 to P2.6) were screened for p_C and the p_L. gRNA P2.3 was selected for further investigation based on very high cleavage efficiency (p_C = 0.997) and predicted loss of function (p_L = 1.0; *SI Appendix*, Fig. S11).

A P2.3 gRNA expression mouse line ($t^{w2\text{-}gRNA}$) was created by targeted integration of a U6-gRNA-mCherry expression cassette at an intergenic site within inversion 1 of the t^{w2} haplotype (43) (Fig. 5 *A* and *B*). We used the early spermatogenesis-specific promoter *Ccna1* (44) to drive Cas9 expression in the male germline (Tg^{Cas9}; Fig. 5 *C* and *D*). $t^{w2\text{-}gRNA/0}$;$Tg^{Cas9/0}$ transhemizygous males (modeling t_{CRISPR}) were mated with wild-type female mice to determine the transmission of the modified *t* haplotype, *Prl* indel efficiency, and the frequency of functional resistant alleles (Fig. 5*E*). Of the 203 F1 embryos sired by transhemizygous males, 142 (p_C = 0.70) contained indels at the target site (range, 0.364 to 0.891 per sire; Table 1), including one sample with biallelic *Prl* mutations, presumably due to Cas9/gRNA carryover (*SI Appendix*, *Supporting Text*). The average number of embryos sired by t_{CRISPR} males (7.8 per pregnant female; Table 1) was not significantly different to the average litter size from t^{w2} sires (7.0; P = 0.262). Next-generation sequencing (NGS) analysis of $t^{w2\text{-}gRNA/0}$;$Tg^{Cas9/0}$ sperm revealed a similarly high indel efficiency (p_C = 0.801, range 0.422 to 0.926 based on 52,427 reads from 10 mice; Table 2). When cutting occurred, the predicted frequency of nonfunctional *Prl* alleles was 1.0. *t* haplotype transmission from $t^{w2\text{-}gRNA}$ males was 0.951, indicating that the transgene insertion did not alter *t* haplotype function. $t^{w2\text{-}gRNA/0}$;$Tg^{Cas9/0}$ females did not display biased transmission of the modified *t* haplotype (p_t = 0.519; Table 1), and no indels were observed in offspring (n = 27), demonstrating that Cas9 activity is confined to males, as expected. Together, these data demonstrate the key properties of the t_{CRISPR} drive, as follows: biased transmission of a modified *t* haplotype and efficient generation and transmission of inactivating mutations in a recessive female fertility gene.

Discussion

Synthetic gene drives have long been proposed for the suppression of invasive alien species and disease vectors. While significant progress has been made in the genetic biocontrol of insects, tools are lacking for mammalian pests. Here, we describe t_{CRISPR}, a population suppression and even eradication strategy for wild mice. Crucially, our transgenic mouse model demonstrates *t* haplotype transmission and associated generation and transmission of inactivating mutations in a recessive female fertility gene, and all are at levels for which our in silico modeling predicts that population eradication can occur.

Table 1. Modified t^{w2} haplotype transmission, p_t, of transhemizygous t_{CRISPR} mice mated with wild-type C57BL/6 mice*

Mouse	No. of pups (no. of litters)	No. of pups with t^{w2}	p_t	No. of pups with *Prl* indel	p_C
Male 1	30 (4)	29	0.967	23	0.767
Male 2	44 (5)	42	0.955	16	0.364
Male 3	46 (5)	41	0.891	41	0.891
Male 4	46 (6)	44	0.957	32	0.696
Male 5	37 (6)	37	1.0	30	0.811
Total	**203 (26)**	**193**	**0.951**	**142**	**0.7**
Female 1	12 (2)	9	0.750	0	0.0
Female 2	15 (2)	5	0.333	0	0.0
Total	**27 (4)**	**14**	**0.519**	**0**	**0.0**

*Pups were screened for P2.3 gRNA p_C. Refer to Dataset S1 for raw data.

Our model predictions indicate that polyandry has a major impact on the spread of t_{CRISPR} (and t^{w2}) and that high levels inhibit t_{CRISPR} population suppression. A similar effect has been observed in a recent study of a wild mouse population containing a different *t* haplotype variant (28). Notably, estimates of multiple paternity in wild mice populations range from 6 to 47% (28, 45–49), which provide reliable lower limits for polyandry estimates; whereas the upper polyandry limit is estimated to be 61% (95% CI: [56 to 65%]) in populations with a lethal *t* haplotype (28). These estimates are within the parameter ranges at which modeling predicts eradication with t_{CRISPR}, suggesting polyandry may not pose a barrier to achieving this management outcome across a range of realistic scenarios. Additional population genetic data, particularly from island cohorts, would further inform t_{CRISPR} eradication potential for wild mice.

Similar to insect homing drives, t_{CRISPR} has little tolerance for functional resistance alleles (so-called r1 resistance alleles). r1 alleles can likely be limited by using gRNAs that target critical amino acid residues, as we have performed. Alternatively, for fertility genes lacking identifiable critical amino acids, multiple gRNAs could be used. Base editing (50, 51) or prime editing (52) platforms could also be employed, as they can generate desired (loss of function) edits without indels, although these approaches would remain susceptible to polymorphic variation at the target locus. Interestingly, our modeling indicates t_{CRISPR} can cause eradication despite incomplete (e.g., 0.80) cleavage efficiency of the female fertility target gene. Unexpectedly, the t_{CRISPR} drive was predicted to be more effective when $p_C = 0.8$ than 1.0. This is similar to other studies showing that if a drive is too efficient, it can rapidly suppress local populations and disappear before having the opportunity to spread (34, 53–56). Close to a 0.80 chance of cleavage was detected in the t_{CRISPR} split drive mouse model, indicating this is feasible. If required, higher cleavage probabilities could likely be achieved using other germline active promoters, noting that Cas9 expression does not need to be restricted to the germline as the target fertility gene is not required in males. The t_{CRISPR} system is also amenable to multiplexed gRNA approaches targeting multiple fertility genes that may offer protection against resistance allele inhibition.

Table 2. *Prl* indel frequency, p_C, and predicted loss of function, p_L from sperm NGS analysis

Mouse	p_C	p_L	Reads
Male 1	0.775	1.0	5,045
Male 2	0.422	1.0	4,997
Male 3	0.819	1.0	6,513
Male 4	0.840	1.0	4,767
Male 5	0.845	1.0	6,313
Male 6	0.874	1.0	4,945
Male 7	0.814	1.0	3,967
Male 8	0.819	1.0	3,967
Male 9	0.882	1.0	7,668
Male 10	0.926	1.0	4,245
Average	**0.801**	**1.0**	**5,243**

Restricting gene drive activity to the targeted population is critically important for ensuring no unintended impacts occur on nontarget populations of the same species, for example in their native range (57). Although islands can provide a natural geographical barrier to unintentional spread, it is generally accepted that multiple safeguards assuring spatial or temporal limitation are required (58, 59). We have recently shown that polymorphisms in female fertility genes that are amenable to SpCas9 cleavage can become fixed in island cohorts (37). These locally fixed alleles could provide potential targets for island-specific t_{CRISPR} strategies (59). Interestingly, our modeling indicates that deployment of t^{w2} during t_{CRISPR}-mediated suppression results in the gradual loss of t_{CRISPR} from the population, suggesting that t^{w2} could potentially be used as a natural (non-genetically modified organism) reversal drive. As such, t^{w2} deployment on the mainland could also serve as a prospective mitigation strategy to prevent nontarget (mainland) population suppression due to escape of t_{CRISPR} drive–carrying mice. Our data also highlight the inhibitory impact of endogenous t^{w2} on t_{CRISPR}-mediated population suppression. Although a *t* variant has been identified in an island population (60), our bioinformatic screening of island/mainland cohorts suggests that it is not common, consistent with published genetic studies of wild populations. The ability of t^{w2} to outcompete t_{CRISPR} also raises an interesting potential susceptibility for t_{CRISPR}-mediated suppression. Spontaneous loss-of-function mutations in either the gRNA or Cas9 coding sequence would effectively convert t_{CRISPR} into t^{w2}-like, potentially inhibiting t_{CRISPR} eradication. Multiplexing gRNA and Cas9 sequences could be used to counter this possibility. This is particularly important as an endogenous failed t_{CRISPR} drive would inhibit a second t_{CRISPR} eradication attempt, even if a different fertility gene was targeted.

Our model predictions for the naturally occurring t^{w2} are in agreement with earlier models showing that t^{w2} can be fixed locally and cause population crashes (25, 26). Compared to t_{CRISPR}, t^{w2} achieved eradication within a much narrower range of parameters and failed as soon as polyandry levels were

moderate. Similar to lethal *t* haplotypes (28–30), the frequencies of t^{w2} were also reduced with increasing levels of polyandry and sperm competition (*SI Appendix*, Fig. S12), which were proposed to be the main contributors to the reduced *t* frequencies observed in nature (28). Alternative explanations, i.e., unreasonably high fitness costs (61) and mate choice against *t* haplotypes (62–64), seem unlikely (28, 65). Encouragingly, t_{CRISPR} is effective under a much wider range of model parameters tolerating higher levels of polyandry, sperm competition, and mate choice compared to t^{w2}.

In summary, we provide in silico modeling and transgenic mouse data supporting a unique strategy for the suppression and even eradication of invasive mice. Although the data are promising, the impact of many empirical factors remains to be explored in detail, including the propensity for t_{CRISPR} introgression (65–68), complexity of deme/population structures, seasonal population variation, unanticipated fitness costs, and possible DNA target site cleavage resistance due to humoral immunity against Cas9 (68). Although genetic biocontrol strategies including gene drives have considerable potential, their development must proceed with utmost caution; be informed by comprehensive risk assessments; have phased testing with a step-by-step approach; and have respectful engagement with stakeholders, publics, and the general community, as well as with regulatory authorities (57, 69). We hope that the advances described here will promote meaningful discussion and debate on the feasibility, benefits, and risks of using gene drives to mitigate the devastating impact of invasive rodents on global biodiversity and the environment.

Materials and Methods

Animal Models. All experiments involving animal use were approved by the South Australian Health & Medical Research Institute (SAHMRI) Animal Ethics Committee.

$t^{P2.3\text{-}gRNA}$ Mouse Generation. To facilitate integration into the *t* haplotype, a t^{int}-gRNA was designed targeting an intergenic locus adjacent to expressed genes within inversion 1 of the *t* haplotype. Complementary gRNA oligos were designed with overhangs facilitating golden gate assembly and cloned into pSpCas9(BB)-2A-Puro (PX459) V2.0 (Addgene plasmid #62988) according to Ran et al. (70). Constructs were validated with a BbsI digest and confirmed by Sanger sequencing. The gRNA was amplified with oligonucleotides containing a 5′ T7 promoter sequence and purified using the QIAquick PCR Purification Kit (Qiagen). RNA was generated using the HiScribe T7 Quick High Yield RNA Synthesis Kit (New England BioLabs [NEB]) followed by purification using the RNeasy MinElute Cleanup Kit (Qiagen).

The donor construct was designed using NEBuilder Assembly Tool (https://nebuilder.neb.com/#!/) to facilitate HiFi assembly. A pBluescript KS(+) plasmid was linearized with EcoRV and the following four fragments were amplified with HiFi compatible overhangs, 1) CMV-mCherry from pZ148-BhCas12b-sgRNA-scaffold (Addgene plasmid #122448), 2) U6-P2.3-HuU6, generated via gBLOCK synthesis (IDT), and 3 and 4) *t* haplotype-specific left and right homology arms from *t*/+ mouse gDNA. Each of these fragments was extracted using a DNA Gel Extraction Kit (NEB) and quantified, and the HiFi reaction was performed as per the manufacturer's protocol using the NEBuilder HiFi DNA Assembly Cloning Kit (NEB). Constructs were verified by a SacII and ClaI digest followed by Sanger sequencing.

Male *t*/+ mice were mated to superovulated C57BL/6 females, and zygotes were harvested. A total of 750 ng Cas9 protein (PNA Bio) and 375 ng integration site gRNA were mixed and incubated on ice for 10 min. A total of 150 ng of donor plasmid was added and the total volume made up to 15 μL with nuclease-free MQ H_2O (Invitrogen). This mix was microinjected into the pronucleus of zygotes followed by oviduct transfer into pseudopregnant females. Transgenic founders were identified by mCherry fluorescence and validated by Sanger sequencing of PCR amplicons from using primer pairs flanking the homology arms (Fig. 5).

Tg^{Cas9} Mouse Generation. The SpCas9-EGFP-bGH poly(A) cassette from Addgene plasmid #61408 was cloned into the pStart-K vector (Addgene #20346). A *Ccna1* promoter region extending 5.7 kb upstream of the start codon (exon 2) was amplified by PCR from C57BL/6 mouse genomic DNA. This region was cloned 5′ of Cas9 in the pStart-K-Cas9-EGFP backbone. An 11.8-kb fragment containing the *Ccna1* promoter fragment, Cas9, EGFP, and bGH poly(A) sequence was digested, gel extracted, and purified. A total of 45 ng of this fragment in 15 μL of 1× microinjection buffer was injected into the pronucleus of zygotes and transferred into pseudopregnant females as described in Bunting et al. (71). A single transgenic founder was confirmed by PCR and further characterized by immunofluorescence, qPCR, and digital PCR (*SI Appendix*, Fig. S11).

Immunofluorescence. Testis immunofluorescence was performed as described (72) using a chicken anti-GFP primary antibody (Abcam, #ab13970) diluted 1/600 and an anti-chicken Alexa Fluor 488 secondary antibody (Thermo Fisher Scientific, #A-11039) diluted 1/300.

t_{CRISPR} Split Drive Analysis. Double hemizygous t_{CRISPR} split drive males were generated by crossing $t^{P2.3\text{-}gRNA}$ and Tg^{Cas9} mice. t_{CRISPR} males were housed with two wild-type C57BL/6 females, who were checked daily for vaginal plugs. Plugged females were removed and replaced with a new wild-type female. Embryos were harvested from pregnant females at 13.5 to 17.5 days post coitum (dpc). Embryonic DNA was extracted using the KAPA Express Extraction kit (Roche) according to the manufacturer's instructions. The P2.3 gRNA target site was amplified, and PCR products were purified by the QIAquick PCR Purification Kit (QIAGEN) and Sanger sequenced. Indel analysis was performed using DECODR (https://decodr.org/). *t* haplotype transmission was assessed by genotyping the Hba-ps4 locus of the *t* allele as described by Schimenti and Hammer (73). Female t_{CRISPR} mice were mated with C57BL/6 males. Ear biopsies from pups were taken at P10, and indel and *t* haplotype transmission was analyzed as above.

To assess *Prl* indel generation in the t_{CRISPR} male germline, sperm from $t^{P2.3\text{-}gRNA/0}/Tg^{Cas9/0}$ mice was isolated from the cauda epididymis using the swim up method. Briefly, extracted sperm was pelleted by centrifugation for 10 min at 360 g. The supernatant was removed and replaced with 10% fetal calf serum + Dulbecco's modified Eagle medium and the sperm pelleted. The tube containing the sperm was placed at a 45° angle in a 37 °C, 5% CO_2 incubator for 1 h followed by removal of the sperm-containing supernatant and centrifugation. Sperm DNA was extracted using the High Pure PCR Template Preparation Kit (Roche), modifying the first step of the protocol. Briefly, pelleted sperm was resuspended in 400 μL tissue lysis buffer and 50 μL of proteinase K and incubated for 1 h at 55 °C. A total of 50 μL of 1M DTT was added, mixed, and incubated overnight at 55 °C. A total of 40 μL of proteinase K was added, and the protocol was continued as per manufacturer's instructions, eluting in 100 μL of elution buffer.

Cell Culture and Transfection. Complementary gRNA oligos were designed with overhangs facilitating golden gate assembly and cloned into pSpCas9(BB)-2A-Puro (PX459) V2.0 (Addgene plasmid #62988) according to Ran et al. (70). R1 Mouse embryonic stem cells were cultured and transfected as described by Adikusuma et al. (74) without modification.

NGS. DNA extracted from $t^{P2.3\text{-}gRNA/0}/Tg^{Cas9/0}$ sperm or mouse embryonic stem cells was amplified with Nextera-tagged primers under standard Phusion PCR conditions. PCR products were sent to the Australian Genome Research Facility for barcoding and paired-end NGS using the MiSeq Nano (500 cycles). NGS reads were analyzed using CRISPResso2 (75) using default parameters except for the following parameters: quantification window size (5bp), minimum average read quality of >20, minimum single bp quality of >10, and bases replaced with N that have a quality lower than <10.

DNA Sequences. Oligonucleotide sequences are listed in *SI Appendix*, Table S2.

In Silico Modeling. The individual-based and spatially explicit modeling framework presented in Birand et al. (34) was used. This is a stochastic, discrete-time model with overlapping generations. Individuals are diploid, have genetically controlled autosomal traits and sex chromosomes, and occupy a rectangular array of patches that together form a hypothetical island. Patches hold multiple individuals and individuals can use multiple patches. Each breeding cycle is

considered a model time step, and individuals that survive long enough pass through a number of breeding cycles until they reach a maximum age (age_m). The number of breeding cycles per year is given by n_c, with the following steps occurring each cycle: 1) mate search, 2) mating, 3) density-dependent reproduction, 4) natal dispersal, 5) survival of adults, and 6) breeding dispersal (*SI Appendix, SI Additional Methods* contains more details).

Suppression and eradication strategies. The *t* haplotype is a naturally occurring segregation distorter with high transmission rates (p_t) to offspring in heterozygous males. The t^{w2} variant causes sterility in homozygous males but has no inheritance biasing or fertility effect in females. We explored the effects of a Cas9/gRNA construct embedded in this variant (hereafter t_{CRISPR}) targeting a fertility gene (e.g., prolactin *Prl*) located on another autosomal chromosome. The fertility gene is present in both sexes but required only in females. The gene is haplosufficient, meaning that when both copies of the gene are deactivated, the female is infertile. We initially assumed that Cas9/gRNA is active in the germline of males only, but we also performed simulations when it is active in the germline of both sexes (denoted $t_{CRISPR(2)}$).

We explored the possibility of evolution of resistance when the fertility gene is cleaved by Cas9/gRNA. The probability of successful fertility gene knockout is given by $p_C p_L$, where p_C is the probability of a successful DNA cut by Cas9/gRNA and p_L is the probability of loss of gene function following a successful cut. We assumed that if the fertility gene retains its function after a cut, it is also resistant to further cuts; therefore, the probability that the resulting allele is functional and resistant is $p_C(1 - p_L)$. The probability of a failed knockout is $(1 - p_C)$, and the allele remains functional and susceptible to further cuts.

We also explored the effect of releasing only naturally occurring t^{w2} variant males without a Cas9/gRNA construct and checked its effectiveness as a population suppression tool via male sterility.

Lastly, we compared the effectiveness of t_{CRISPR} as a suppression and eradication strategy with the homing and X-shredding drives, which were investigated in detail by Birand et al. (34). The homing drive is a CRISPR-based drive that is positioned in an exon of the same female fertility gene targeted by t_{CRISPR} and generates a loss-of-function mutation. The X-shredding drive is a CRISPR-based drive located on the Y chromosome and cuts the X chromosome with probability p_x at multiple locations beyond repair during spermatogenesis. Since X-bearing sperm are destroyed and eggs are predominantly fertilized by Y-bearing sperm, the drive causes disproportionately more male offspring.

Parameters and initial conditions. Life history and demography parameters (*SI Appendix*, Table S1) are based on empirical data whenever available (for details, see Birand et al. (34)). We use the same spatial configuration provided in Birand et al. (34), as follows: $64 \times 64 = 4{,}096$ patches in the model corresponds to a 70-m × 70-m space on a hypothetical island of ∼2,000 ha. We calibrated dispersal abilities on this island based on historical invasion records of a similar sized island (76); maximum dispersal distances $D = [4,7]$ in the model correspond to 240 to 560m in the wild (77, 78). We assumed that the population size was ∼200,000 before inoculation.

After a burn-in period of 2 y, the simulated island is inoculated with males carrying *t* haplotype variants (t_{CRISPR} or t^{w2}) detailed above. We modeled a single release into 256 patches distributed systematically across the island, with 1 male ($N_i = 1$) with t_{CRISPR} or t^{w2} released into each patch (total of 256 males), assuming that would be an achievable release size. Releasing more individuals with gene drives reduces the simulated time to eradication [e.g., Birand et al. (79)]. Following their release, *t*-carrying mice randomly choose a patch within distance *D* from their inoculation patches and join the pool of available males for mating. Females choose males randomly among all the available males, which implies that some *t* haplotype–carrying males may not be chosen for mating (potentially more so if there is mate choice against *t* haplotype males by *t* haplotype females).

We ran simulations for a maximum of 500 breeding cycles (i.e., 81 y after inoculation) and compared the efficacy of different gene-drive strategies under different parameter assumptions. We also performed a global sensitivity analysis for each suppression strategy to investigate the relative influence of parameters on the probability of successful eradication and the time to eradication (see below), in addition to brute force simulations with certain parameter combinations. The model is coded using C programming language and is available from the Zenodo Open Repository (10.5281/zenodo.6583793).

Sensitivity analysis. We performed a global sensitivity analysis for each suppression strategy to investigate the relative influence of parameters on the probability of successful eradication and the time to eradication. In each case, we created 3,000 unique parameter combinations from parameter ranges given in *SI Appendix*, Table S1 using Latin hypercube sampling [randomLHS, R package (80)]. In order to minimize computational effort and maximize the coverage of the parameter space, we ran a single simulation for each parameter combination (81). Finally, we examined the influence of parameter inputs using Boosted Regression Tree models [BRTs; R package *dismo* (82)] that we fitted to the simulation outputs using the function gbm.step from the R package *dismo* [learning rate: 0.01; bag fraction: 0.75; tree complexity: 3; and fivefold cross-validation (83)].

We used binomial error distribution for the probability of eradication, and Poisson error distribution for time to eradication (83). We labeled simulation outcomes as unsuccessful for the binomial error distribution if eradication did not occur within the number of breeding cycles simulated, even when the population was suppressed to a new stable level. To investigate the influence of parameters on the time to eradication, we only used simulations when eradication was achieved.

Presence of *t* Haplotypes on Islands. To assess the presence of *t* haplotypes in island mice, we analyzed previously published pool-seqs from four introduced populations on islands in Western Australia (Whitlock-Boulanger Islands and Thevenard Island), the northern Pacific (Sand Island in Midway Atoll), and North America (South Farallon Island) (37). As it is generally not possible to extract haplotype information from pool-seq data, we used an approach wherein sequencing reads were mapped to a reference of diagnostic *t*-specific transcripts. These reference transcripts were derived from results of a recent study by Kelemen et al. (84) that analyzed DNA and RNA sequences from a database of wild *Mus* samples (85). This database includes whole-genome sequences from both +/*t* and $^{+/+}$ mice across all three *M. musculus* subspecies as well as a sister taxon (*Mus spretus*). The original list [Supplementary Data 4 in Kelemen et al. (84)] consists of 256 annotated contigs assembled from RNA-seq reads of +/*t* mice and subsequently filtered for those that had greater relative coverage of genomic reads mapped from +/*t* compared to $^{+/+}$ mice.

In order to identify diagnostic *t*-specific transcripts for our study, we downloaded DNA sequence FASTQ files for +/*t* and $^{+/+}$ mice from the Harr et al. (85) database and remapped the forward reads of each sample to the transcripts using Bowtie 2 (86). Following the procedure by Kelemen et al. (84), we then counted only reads that mapped perfectly to a transcript with no mismatches and normalized these values by the total number of reads in each sequence dataset, multiplied by 1×10^6 to calculate reads per million. Diagnostic *t*-specific transcripts were then identified as those to which zero reads mapped from any $^{+/+}$ individuals and at least one read mapped in each +/*t* sample. This final list of transcripts was then used to screen island pool-seq data for the presence of *t* haplotypes in each population. At the same time, we also analyzed the four source mouse populations from the same study as a control (37), as some have speculated that *t*-alleles may tend to be more common in larger populations that are less influenced by genetic drift (87). We downloaded the FASTQ files for each pool-seq dataset from the NCBI Short Read Archive (Bioproject PRJNA702596) and mapped the first reads to the set of diagnostic *t*-transcripts as above and calculated the fraction of transcripts with at least one read mapped as well as the normalized counts of reads mapped.

As our primary aim was to evaluate the presence or absence of *t* haplotypes in each island population, we compared observed *t*-specific read counts to the expected values under a scenario where a single *t* haplotype-bearing chromosome was sampled within the pool-seq experiment. To simulate this, we concatenated FASTQ files from +/*t* samples in the Harr et al. (85) database and randomly subsampled using rasusa (88) down to a coverage equal to $1n \times C$, where *n* and *C* are the number of haploid genomes sampled in each empirical pool-seq sample and the total library sequencing coverage (first reads only), respectively [*SI Appendix*, Table S3; Oh et al. (37)]. The process was repeated with a concatenated FASTQ file of reads from $^{+/+}$ samples, subsampled to $(n - 1)n \times C$, and then both files were combined and mapped to the diagnostic *t*-specific transcripts as above to generate expected counts. Each simulation was iterated 100 times in each population to generate mean expected values and 95% confidence intervals.

We note that our analyses assume an equal contribution of each individual sample within the pool-seq libraries. Violation of this assumption could lead to under- or overrepresentation of reads mapping to *t*-specific transcripts in the data, although the original study (37) adopted best practices (89) to minimize such biases (e.g., DNA was quantified fluorometrically in triplicate prior to pooling).

Data, Materials, and Software Availability. The code for the individual-based model is available from the Zenodo Open Repository (https://doi.org/10.5281/zenodo.6583793) (90).

ACKNOWLEDGMENTS. We thank Dan Tompkins and members of the Genetic Biocontrol of Invasive Rodents (GBIRd) consortium for commenting on the manuscript. The findings and conclusions in this publication are those of the authors and should not be construed to represent any official US Department of Agriculture (USDA) or US Government determination or policy. Figs. 1 and 5 and SI Appendix, Fig. S11 were created using BioRender.com. This research was supported by the Government of New South Wales, the Centre for Invasive Species Solutions, and the Government of South Australia. This research was also supported in part by the USDA Animal Plant Inspection Service, Wildlife Services, National Wildlife Research Center. The authors acknowledge the facilities and the scientific and technical assistance of the South Australian Genome Editing (SAGE) Facility, the University of Adelaide, and the South Australian Health and Medical Research Institute. SAGE is supported by Phenomics Australia. Phenomics Australia is supported by the Australian Government through the National Collaborative Research Infrastructure Strategy (NCRIS) program. This work was also supported with supercomputing resources provided by the Phoenix High Performance Computing (HPC) service at the University of Adelaide.

Author affiliations: [a]School of Biomedicine and Robinson Research Institute, University of Adelaide, Adelaide, SA 5000, Australia; [b]Genome Editing Program, South Australian Health and Medical Research Institute, Adelaide, SA 5000, Australia; [c]Invasion Science and Wildlife Ecology Lab, School of Biological Sciences, The University of Adelaide, Adelaide, SA 5000, Australia; [d]Australian Centre for Disease Preparedness, CSIRO Health and Biosecurity, Geelong, VIC 3220, Australia; [e]Applied BioSciences, Macquarie University, North Ryde, NSW 2614, Australia; [f]CSIRO Health and Biosecurity, Canberra, ACT 2601, Australia; [g]United States Department of Agriculture, Animal Plant Health Inspection Service, Wildlife Services, National Wildlife Research Center, Fort Collins, CO 80521; [h]Department of Cell Biology and Genetics, Texas A&M University, College Station, TX 76549; [i]Department of Biological Sciences and Genetic Engineering and Society Center, North Carolina State University, Raleigh, NC 27695; [j]CSIRO Land & Water, CSIRO Synthetic Biology Future Science Platform, Perth, WA 6014, Australia; and [k]School of Mathematical Sciences, The University of Adelaide, Adelaide, SA 5000, Australia

1. T. S. Doherty, A. S. Glen, D. G. Nimmo, E. G. Ritchie, C. R. Dickman, Invasive predators and global biodiversity loss. *Proc. Natl. Acad. Sci. U.S.A.* **113**, 11261–11265 (2016).
2. P. Pyšek *et al.*, Scientists' warning on invasive alien species. *Biol. Rev. Camb. Philos. Soc.* **95**, 1511–1534 (2020).
3. D. R. Paini *et al.*, Global threat to agriculture from invasive species. *Proc. Natl. Acad. Sci. U.S.A.* **113**, 7575–7579 (2016).
4. J. Godwin *et al.*, Rodent gene drives for conservation: Opportunities and data needs. *Proc. Biol. Sci.* **286**, 20191606 (2019).
5. T. M. Blackburn, P. Cassey, R. P. Duncan, K. L. Evans, K. J. Gaston, Avian extinction and mammalian introductions on oceanic islands. *Science* **305**, 1955–1958 (2004).
6. M. Clavero, E. García-Berthou, Invasive species are a leading cause of animal extinctions. *Trends Ecol. Evol.* **20**, 110 (2005).
7. H. P. Jones *et al.*, Invasive mammal eradication on islands results in substantial conservation gains. *Proc. Natl. Acad. Sci. U.S.A.* **113**, 4033–4038 (2016).
8. J. C. Russell, C. Kueffer, Island biodiversity in the anthropocene. *Annu. Rev. Environ. Resour.* **44**, 31–60 (2019).
9. C. Bellard, P. Cassey, T. M. Blackburn, Alien species as a driver of recent extinctions. *Biol. Lett.* **12**, 20150623 (2016).
10. F. Courchamp, J. L. Chapuis, M. Pascal, Mammal invaders on islands: Impact, control and control impact. *Biol. Rev. Camb. Philos. Soc.* **78**, 347–383 (2003).
11. E. Bier, Gene drives gaining speed. *Nat. Rev. Genet.* **23**, 5–22. (2021).
12. A. Burt, Site-specific selfish genes as tools for the control and genetic engineering of natural populations. *Proc. Biol. Sci.* **270**, 921–928 (2003).
13. S. P. Sinkins, F. Gould, Gene drive systems for insect disease vectors. *Nat. Rev. Genet.* **7**, 427–435 (2006).
14. M. Jinek *et al.*, A programmable dual-RNA-guided DNA endonuclease in adaptive bacterial immunity. *Science* **337**, 816–821 (2012).
15. N. Windbichler *et al.*, A synthetic homing endonuclease-based gene drive system in the human malaria mosquito. *Nature* **473**, 212–215 (2011).
16. V. M. Gantz *et al.*, Highly efficient Cas9-mediated gene drive for population modification of the malaria vector mosquito *Anopheles stephensi*. *Proc. Natl. Acad. Sci. U.S.A.* **112**, E6736–E6743 (2015).
17. A. Hammond *et al.*, A CRISPR-Cas9 gene drive system targeting female reproduction in the malaria mosquito vector Anopheles gambiae. *Nat. Biotechnol.* **34**, 78–83 (2016).
18. K. Kyrou *et al.*, A CRISPR-Cas9 gene drive targeting doublesex causes complete population suppression in caged *Anopheles gambiae* mosquitoes. *Nat. Biotechnol.* **36**, 1062–1066 (2018).
19. H. A. Grunwald *et al.*, Super-Mendelian inheritance mediated by CRISPR-Cas9 in the female mouse germline. *Nature* **566**, 105–109 (2019).
20. C. Pfitzner *et al.*, Progress toward zygotic and germline gene drives in mice. *CRISPR J.* **3**, 388–397 (2020).
21. A. J. Weitzel *et al.*, Meiotic Cas9 expression mediates gene conversion in the male and female mouse germline. *PLoS Biol.* **19**, e3001478 (2021).
22. N. Dobrovolskaia-Zavadskaia, Sur la mortification spontanee de la queuw chez la spuris nouveau et sur l'existence d'un caractere (facteur) hereditaire non viable. *Compr. Soc. Biol.* **97**, 114–119 (1927).
23. D. Bruck, Male segregation ratio advantage as a factor in maintaining lethal alleles in wild populations of house mice. *Proc. Natl. Acad. Sci. U.S.A.* **43**, 152–158 (1957).
24. L. M. Silver, Mouse t haplotypes. *Annu. Rev. Genet.* **19**, 179–208 (1985).
25. L. C. Dunn, H. Levene, Population dynamics of a variant *t*-allele in a confined population of wild house mice. *Evolution* **15**, 385 (1961).
26. R. C. Lewontin, Interdeme selection controlling a polymorphism in the house mouse. *Am. Nat.* **96**, 65 (1962).
27. S. Lenington, P. Franks, J. Williams, Distribution of *T*-haplotypes in natural populations of wild house mice. *J. Mammal.* **69**, 489–499 (1988).
28. A. Manser, B. König, A. K. Lindholm, Polyandry blocks gene drive in a wild house mouse population. *Nat. Commun.* **11**, 5590 (2020).
29. A. Manser, A. K. Lindholm, B. König, H. C. Bagheri, Polyandry and the decrease of a selfish genetic element in a wild house mouse population. *Evolution* **65**, 2435–2447 (2011).
30. A. Manser, A. K. Lindholm, L. W. Simmons, R. C. Firman, Sperm competition suppresses gene drive among experimentally evolving populations of house mice. *Mol. Ecol.* **26**, 5784–5792 (2017).
31. A. Manser *et al.*, Controlling invasive rodents via synthetic gene drive and the role of polyandry. *Proc. Biol. Sci.* **286**, 20190852 (2019).
32. N. D. Horseman *et al.*, Defective mammopoiesis, but normal hematopoiesis, in mice with a targeted disruption of the prolactin gene. *EMBO J.* **16**, 6926–6935 (1997).
33. D. Bennett, The T-locus of the mouse. *Cell* **6**, 441–454 (1975).
34. A. Birand *et al.*, Gene drives for vertebrate pest control: Realistic spatial modelling of eradication probabilities and times for island mouse populations. *Mol. Ecol.* **31**, 1907–1923 (2022).
35. T. A. Prowse, F. Adikusuma, P. Cassey, P. Thomas, J. V. Ross, A Y-chromosome shredding gene drive for controlling pest vertebrate populations. *eLife* **8**, e41873 (2019).
36. J. Champer, I. K. Kim, S. E. Champer, A. G. Clark, P. W. Messer, Suppression gene drive in continuous space can result in unstable persistence of both drive and wild-type alleles. *Mol. Ecol.* **30**, 1086–1101 (2021).
37. K. P. Oh *et al.*, Population genomics of invasive rodents on islands: Genetic consequences of colonization and prospects for localized synthetic gene drive. *Evol. Appl.* **14**, 1421–1435 (2021).
38. S. Kinet, V. Goffin, V. Mainfroid, J. A. Martial, Characterization of lactogen receptor-binding site 1 of human prolactin. *J. Biol. Chem.* **271**, 14353–14360 (1996).
39. D. N. Luck *et al.*, Analysis of disulphide bridge function in recombinant bovine prolactin using site-specific mutagenesis and renaturation under mild alkaline conditions: A crucial role for the central disulphide bridge in the mitogenic activity of the hormone. *Protein Eng.* **5**, 559–567 (1992).
40. D. N. Luck, M. Huyer, P. W. Gout, C. T. Beer, M. Smith, Single amino acid substitutions in recombinant bovine prolactin that markedly reduce its mitogenic activity in Nb2 cell cultures. *Mol. Endocrinol.* **5**, 1880–1886 (1991).
41. I. Broutin *et al.*, Crystal structure of an affinity-matured prolactin complexed to its dimerized receptor reveals the topology of hormone binding site 2. *J. Biol. Chem.* **285**, 8422–8433 (2010).
42. G. V. Rao, C. L. Brooks, Functional epitopes for site 1 of human prolactin. *Biochemistry* **50**, 1347–1358 (2011).
43. D. M. Kanavy, *Genetic Pest Management Technologies to Control Invasive Rodents* (North Carolina State University, 2018).
44. K. M. Lele, D. J. Wolgemuth, Distinct regions of the mouse cyclin A1 gene, Ccna1, confer male germ-cell specific expression and enhancer function. *Biol. Reprod.* **71**, 1340–1347 (2004).
45. L. S. Carroll, S. Meagher, L. Morrison, D. J. Penn, W. K. Potts, Fitness effects of a selfish gene (the *Mus t* complex) are revealed in an ecological context. *Evolution* **58**, 1318–1328 (2004).
46. M. D. Dean, K. G. Ardlie, M. W. Nachman, The frequency of multiple paternity suggests that sperm competition is common in house mice (*Mus domesticus*). *Mol. Ecol.* **15**, 4141–4151 (2006).
47. R. C. Firman, L. W. Simmons, The frequency of multiple paternity predicts variation in testes size among island populations of house mice. *J. Evol. Biol.* **21**, 1524–1533 (2008).
48. I. Montero, M. Teschke, D. Tautz, Paternal imprinting of mating preferences between natural populations of house mice (*Mus musculus domesticus*). *Mol. Ecol.* **22**, 2549–2562 (2013).
49. K. E. Thonhauser, M. Thoß, K. Musolf, T. Klaus, D. J. Penn, Multiple paternity in wild house mice (*Mus musculus musculus*): Effects on offspring genetic diversity and body mass. *Ecol. Evol.* **4**, 200–209 (2014).
50. N. M. Gaudelli *et al.*, Programmable base editing of A•T to G•C in genomic DNA without DNA cleavage. *Nature* **551**, 464–471 (2017).
51. A. C. Komor, Y. B. Kim, M. S. Packer, J. A. Zuris, D. R. Liu, Programmable editing of a target base in genomic DNA without double-stranded DNA cleavage. *Nature* **533**, 420–424 (2016).
52. A. V. Anzalone *et al.*, Search-and-replace genome editing without double-strand breaks or donor DNA. *Nature* **576**, 149–157 (2019).
53. P. A. Eckhoff, E. A. Wenger, H. C. J. Godfray, A. Burt, Impact of mosquito gene drive on malaria elimination in a computational model with explicit spatial and temporal dynamics. *Proc. Natl. Acad. Sci. U.S.A.* **114**, E255–E264 (2017).
54. A. R. North, A. Burt, H. C. J. Godfray, Modelling the potential of genetic control of malaria mosquitoes at national scale. *BMC Biol.* **17**, 26 (2019).
55. A. North, A. Burt, H. C. J. Godfray, Modelling the spatial spread of a homing endonuclease gene in a mosquito population. *J. Appl. Ecol.* **50**, 1216–1225 (2013).
56. S. E. Champer *et al.*, Modeling CRISPR gene drives for suppression of invasive rodents using a supervised machine learning framework. *PLOS Comput. Biol.* **17**, e1009660 (2021).

57. K. C. Long *et al.*, Core commitments for field trials of gene drive organisms. *Science* **370**, 1417–1419 (2020).
58. J. Champer *et al.*, Molecular safeguarding of CRISPR gene drive experiments. *eLife* **8**, e41439 (2019).
59. J. Sudweeks *et al.*, Locally fixed alleles: A method to localize gene drive to island populations. *Sci. Rep.* **9**, 15821 (2019).
60. G. B. Dooher, R. J. Berry, K. Artzt, D. Bennett, A semilethal *t*-haplotype in the Orkney Islands. *Genet. Res.* **37**, 221–226 (1981).
61. R. C. Lewontin, The effect of differential viability on the population dynamics of *t* alleles in the house mouse. *Evolution* **22**, 262–273 (1968).
62. S. Lenington, C. Coopersmith, J. Williams, Genetic basis of mating preferences in wild house mice. *Am. Zool.* **32**, 40–47 (1992).
63. A. Manser, B. König, A. K. Lindholm, Female house mice avoid fertilization by *t* haplotype incompatible males in a mate choice experiment. *J. Evol. Biol.* **28**, 54–64 (2015).
64. A. Sutter, A. K. Lindholm, No evidence for female discrimination against male house mice carrying a selfish genetic element. *Curr. Zool.* **62**, 675–685 (2016).
65. M. Serr, N. Heard, J. Godwin, "Island invasives: Scaling up to meet the challenge" in *Proceedings of the international conference on island invasives 2017* (Gland, Switzerland, 2017).
66. P. K. Anderson, L. C. Dunn, A. B. Beasley, Introduction of a lethal allele into a feral house mouse population. *Am. Nat.* **98**, 57–64 (1964).
67. P. R. Pennycuik, P. G. Johnston, W. Z. Lidicker, N. H. Westwood, Introduction of a male sterile allele (*Tw2*) into a population of house mice housed in a large outdoor enclosure. *Aust. J. Zool.* **26**, 69–81 (1978).
68. C. T. Charlesworth *et al.*, Identification of preexisting adaptive immunity to Cas9 proteins in humans. *Nat. Med.* **25**, 249–254 (2019).
69. Committee on Gene Drive Research in Non-Human Organisms: Recommendations for Responsible *et al.*, "Gene drives on the horizon: Advancing science, navigating uncertainty, and aligning research with public values" in *Gene Drives on the Horizon: Advancing Science, Navigating Uncertainty, and Aligning Research with Public Values* (National Academies Press, Washington, DC, 2016), 10.17226/23405.
70. F. A. Ran *et al.*, Genome engineering using the CRISPR-Cas9 system. *Nat. Protoc.* **8**, 2281–2308 (2013).
71. M. D. Bunting *et al.*, Generation of gene drive mice for invasive pest population suppression. *Methods Mol. Biol.* **2495**, 203–230 (2022).
72. D. McAninch *et al.*, SOX3 promotes generation of committed spermatogonia in postnatal mouse testes. *Sci. Rep.* **10**, 6751 (2020).
73. J. Schimenti, M. Hammer, Rapid identification of mouse t haplotypes by PCR polymorphism (PCRP). *Mouse Genome* **87**, 108 (1990).
74. F. Adikusuma *et al.*, Optimized nickase- and nuclease-based prime editing in human and mouse cells. *Nucleic Acids Res.* **49**, 10785–10795 (2021).
75. K. Clement *et al.*, CRISPResso2 provides accurate and rapid genome editing sequence analysis. *Nat. Biotechnol.* **37**, 224–226 (2019).
76. R. Taylor, *Straight through from London: The Antipodes and Bounty Islands, New Zealand/Rowley Taylor* (Heritage Expeditions New Zealand, Christchurch, NZ, 2006).
77. H. W. Nathan, M. N. Clout, J. W. B. MacKay, E. C. Murphy, J. C. Russell, Experimental island invasion of house mice. *Popul. Ecol.* **57**, 363–371 (2015).
78. D. Moro, K. Morris, Movements and refugia of Lakeland Downs short-tailed mice, Leggadina lakedownensis, and house mice, *Mus domesticus*, on Thevenard Island, Western Australia. *Wildl. Res.* **27**, 11–20 (2000).
79. A. Birand, P. Cassey, J. V. Ross, P. Q. Thomas, T. A. A. Prowse, Scalability of genetic biocontrols for eradicating invasive alien mammals. *NeoBiota* **74**, 93–103 (2022).
80. R. Carnell, lhs: Latin hypercube samples (2022). https://CRAN.R-project.org/package=lhs. Accessed 23 March 2022.
81. T. A. A. Prowse *et al.*, An efficient protocol for the global sensitivity analysis of stochastic ecological models. *Ecosphere* **7**, e01238 (2016).
82. R. J. Hijmans, S. Phillips, J. Leathwick, J. Elith, Dismo: Species Distribution Modeling. R Package Version 1.0-12 (2015). cran.r-project.org/web/packages/dismo/index.html. Accessed 23 March 2022.
83. J. Elith, J. R. Leathwick, T. Hastie, A working guide to boosted regression trees. *J. Anim. Ecol.* **77**, 802–813 (2008).
84. R. K. Kelemen, M. Elkrewi, A. K. Lindholm, B. Vicoso, Novel patterns of expression and recruitment of new genes on the *t*-haplotype, a mouse selfish chromosome. *Proc. Biol. Sci.* **289**, 20211985 (2022).
85. B. Harr *et al.*, Genomic resources for wild populations of the house mouse, *Mus musculus* and its close relative *Mus spretus*. *Sci. Data* **3**, 160075–160075 (2016).
86. B. Langmead, S. L. Salzberg, Fast gapped-read alignment with Bowtie 2. *Nat. Methods* **9**, 357–359 (2012).
87. D. Bennett, "*Population genetics of T/t complex mutations*" in *Origins of Inbred Mice*, H. C. Morse, Ed. (Academic Press, New York, 1978), pp. 615–632.
88. M. B. Hall, Rasusa: Randomly subsample sequencing reads to a specified coverage. *J. Open Source Softw.* **7**, 3941 (2022).
89. N. O. Rode *et al.*, How to optimize the precision of allele and haplotype frequency estimates using pooled-sequencing data. *Mol. Ecol. Resour.* **18**, 194–203 (2018).
90. A. Birand, P. Cassey, J. V. Ross, T. A. A. Prowse, P. Q. Thomas, Leverating a natural murine meiotic drive to suppress invasive populations. Zenodo. https://doi.org/10.5281/zenodo.6583793. Deposited 26 May 2022.